Earth Reinforcement Practice, Ochiai, Hayashi & Otani (eds) © 1992 Balkema, Rotterdam. ISBN 90 5410 093 1

Loading tests of geosynthetic-reinforced soil retaining walls and their stability analyses

O. Murata & M. Tateyama
Railway Technical Research Institute, Kokubunji, Japan

F. Tatsuoka
Institute of Industrial Science, University of Tokyo, Japan

ABSTRACT: Four full-scale test geosynthetic-reinforced soil retaining walls with a sand or clay backfill reinforced with a relatively short geotextile (about 30% wall height) having a continuous rigid facing were loaded to failure with a large footing on the crest. In the laboratory, static and dynamic loading tests were performed on scaled models with a reinforced backfill sand having a facing with different degrees of rigidity. The models became more stable as the facing rigidity increased. This result was successfully simulated by limit equilibrium stability analyses based on the experimental finding that the facing rigidity increases the earth pressure on the facing back face and locates the total reaction activated on the bottom of facing and backfill closer to the toe of facing.

1 INTRODUCTION

A permanent geosynthetic-reinforced soil (GRS) retaining wall system which satisfies the following requirements has been developed by using relatively short sheets of geosythetic and a continuous rigid facing (Murata et al., 1991, Tatsuoka et al., 1991, 1992): **A)** By using an appropriate type of geosythetic, it should permit the usage of most on-site soils as the backfill soil, which leads to a considerably large cost saving, compared with the cost for the use of selected cohesionless soil and the treatment of excavated soil. **B)** It can reconstruct a gentle slope of existing embankment to a near vertical or vertical wall without a large amount of excavation (Fig. 1). **C)** It should exhibit very small deformation, especially very small settlement at the crest so as to use as important permanent structures such as bridge abutments supporting vertical and horizontal loads acting on the crest near the wall face. **D)** It should be reasonably inexpensive so as to use for large lengths as, for instance, railway or highway embankments. **E)** To achieve a relatively long lifetime, the wall face should be sufficiently durable against natural and artificial damaging actions. **F)** The wall face should be aesthetically acceptable, which is particularly important when constructed in an urban area. Potential damage due to the relative settlement between the rigid facing and the backfill can be avoided by using a delayed cast-in-place concrete facing. This wall system has already been used to reconstruct slopes of railway embankment for almost 7km. This paper presents the results of model tests and stability analyses taking into account the effect of facing rigidity.

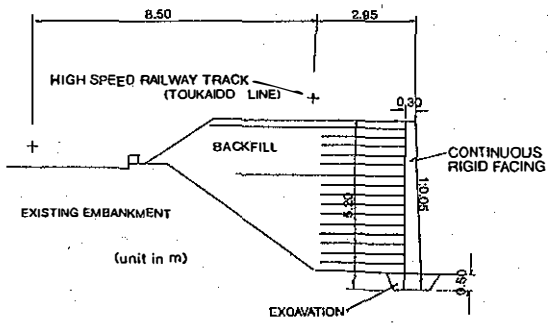

Fig. 1 Typical railway embankment slope reconstructed by the proposed GRS retaining wall system, Amagasaki.

2 LOADING TESTS OF GRS RETAINING WALLS

In the laboratory, 50cm-high GRS retaining walls with sand backfill reinforced with a model grid having different types of facing with various degrees of rigidity were constructed (Fig. 2). Type **A** facing was made of rubber membrane. Type **B'** was made of tracing paper, which was stiffer than Type **A**. Type **B** was made by piling up wooden blocks having a smooth back face with a soft material in between vertically adjacent blocks so as to reduce the facing rigidity as the French Reinforced Earth retaining walls. Type **C** was similar to Type

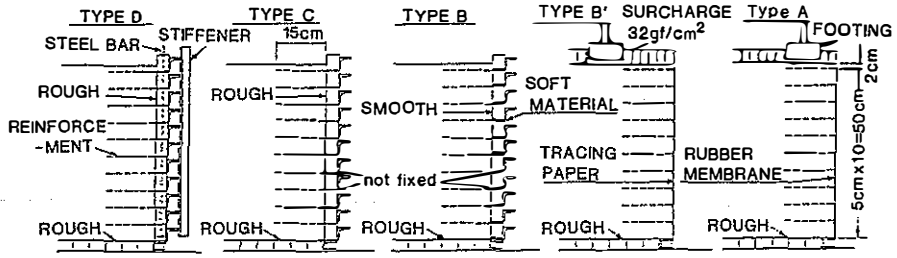

Fig. 2 Small models of GRS retaining wall in the laboratory (Tatsuoka et al., 1989).

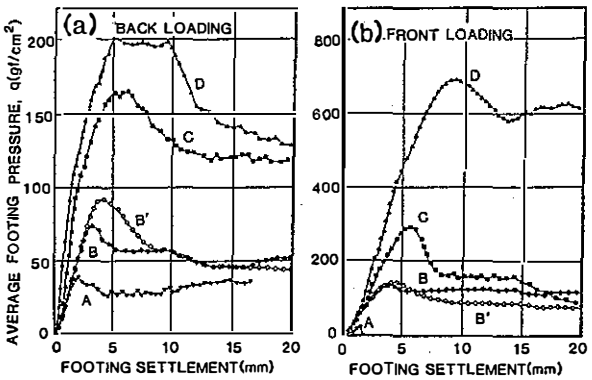

Fig. 3 Average footing pressure versus footing settlement for the models (Fig. 2); (a) Back loading and (b) front loading (Tatsuoka et al., 1989).

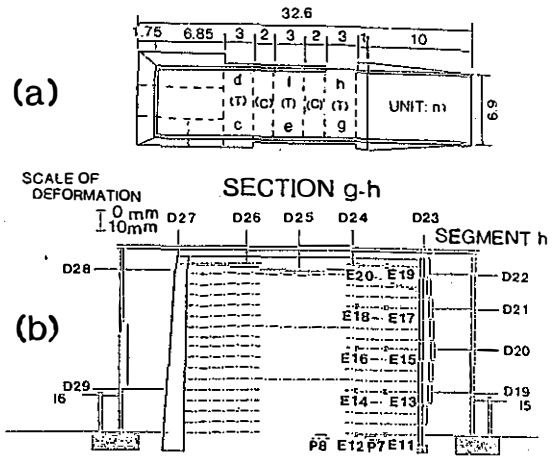

Fig. 4 (a) Plan (T; test section, and C; control section) and (b) one section of No. 1 embankment (sand).

B, but the back face was made rough and the blocks were in direct contact with each other. For Type D, the wooden blocks were tightly fixed to form a continuous rigid facing. These model walls were loaded to failure by means of a 10cm-wide strip footing with a smooth base. For each type of wall, front loading (loading from the top of the reinforced zone, see the right-most figure in Fig. 2) and back loading (loading from immediately behind the reinforced zone) were performed (Fig. 3). In each case, the wall was more stable in the order of Types D, C, B, B' and A in accordance with the degree of facing rigidity. In particular, despite the use of relatively short reinforcement (only 30% the wall height), the model wall using a continuous rigid facing of Type D was very stable.

Two full-scale test embankments Nos. 1 and 2 were constructed in 1988 and 1989 by using sand and clay, respectively, as the backfill soil. Herein, only No.1 embankment will be described. The backfill sand had D_{50}= 0.2mm and a fines content of 16%. In Fig. 4, the solid and broken lines show the dimensions at the end of construction and about two years after construction, respectively. The vertical spacing between reinforcement layers was 30cm and the length of reinforcement was 2.0m, except 1.5m for Segment f. The test wall segments had a delayed cast-in-place unreinforced concrete facing with two lightly reinforced construction joints having a slightly inclined wall face, except Segment h having a discrete panel facing (Type C, Fig. 2). The backfill was reinforced with a grid having a tensile rupture strength of 2.8tonf/m and an initial modulus of 1.0tonf/m at an elongation of 5%. All the wall segments having a continuous rigid facing exhibited a very small settlement of 1cm or less even at the center of crest over one and a half years (Fig. 4), whereas Segment h having a discrete-panel facing deformed much more largely.

Three segments of No.1 embankment were loaded from their crests using a 2m x 3m footing (Fig. 5). These 3m-wide test sections were separated from each other through a 2m-wide control section in between by using a layer of two plywood sheets sandwiching a layer of grease used to lubricate the boundary planes. The footing was located at a setback of 2m from the crest edge of Segments d, f and h (Fig. 6). Fig. 7 shows the average footing pressure plotted against the horizontal outward displacement at the mid-height of facing, which is representative of the defor-

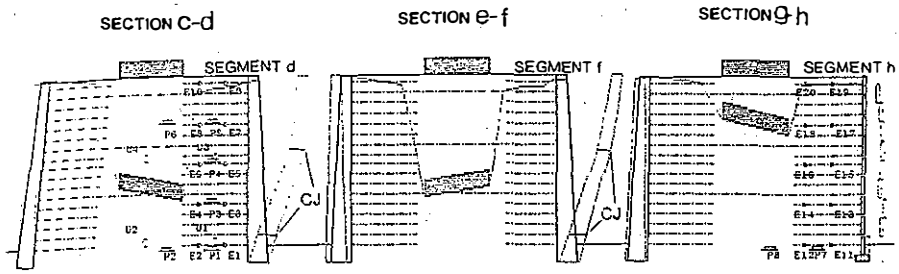

SEGMENT	d	f	h
SETTLEMENT OF FOOTING (cm)	69.4	68.3	29.8
FOOTING PRESSURE (tonf/m²)	57.5	50.0	37.5

SCALE OF DEFORMATION
10 cm

Fig. 6 Deformation of three sections of No.1 embankment by back loading test.

mation of facing. The effect of the different lengths of geotextile between Segments d and f (2.0m and 1.5m) and the effect of the different facing types between Segments d and h may be clearly seen. The very low part of the discrete-panel facing of Segment h buckled during loading (Fig. 6), since the facing could not resist large axial force in the facing during loading. Segments d and f yielded when a crack appeared in the upper construction joint of facing (Fig. 6). Therefore, if the construction joints had been stronger, the strength of the walls would have been larger. One section of No. 2 embankment was also loaded to failure (Murata et al., 1991, Tatsuoka et al., 1992).

For the aseismic design of the GRS retaining wall system, five 100cm-high models were constructed on a shaking table (Fig. 8). The sand backfill was reinforced with a grid having a high rupture strength of 1.0tf/m, which leaded to no chance of rupture during the model tests. Model 1 was the standard one having a vertical continuous rigid facing (Type D). Compared to Model 1, Model 5 had a discrete panel facing (Type B), Models 2 had longer reinforcement, Model 3 had an inclined facing and Model 4 had a smaller number of reinforcement layers. A series of horizontal shaking at a constant amplitude of acceleration was applied with increasing the acceleration level step by step. The accumulated horizontal outward displacement of facing at the end of each step of shaking was much larger for Model 5 than for Model 1 (Fig. 9), apparently due to its low facing rigidity. The wall also became more stable by using longer reinforcement (Model 2) and by using an inclined facing (Model 3), but became less stable by using a smaller number of reinforcement layers (Model 4). Further, a 2.48m-high model of No.1 embankment constructed on a large shaking table was dynamically loaded. The test results using these small and large models showed

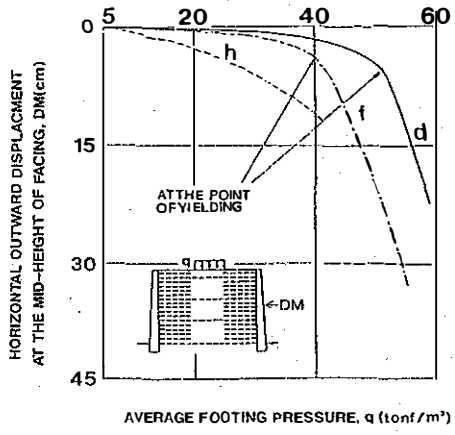

Fig. 7 Load-displacement relations for Segments d, f and h, No. 1 embankment; the average pressure by the weight of the loading apparatus = 5tonf/m².

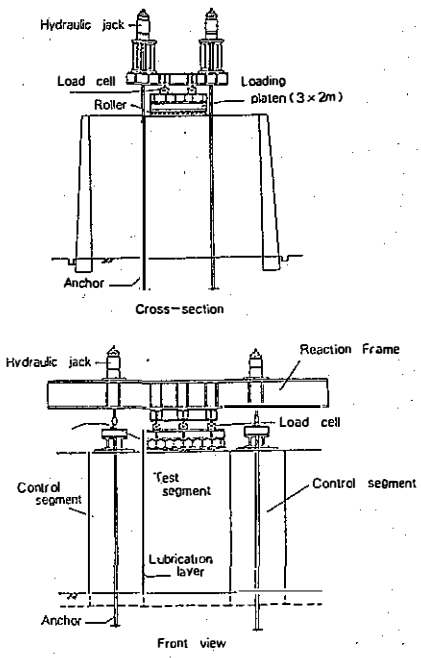

Fig. 5 Back loading for No. 1 embankment.

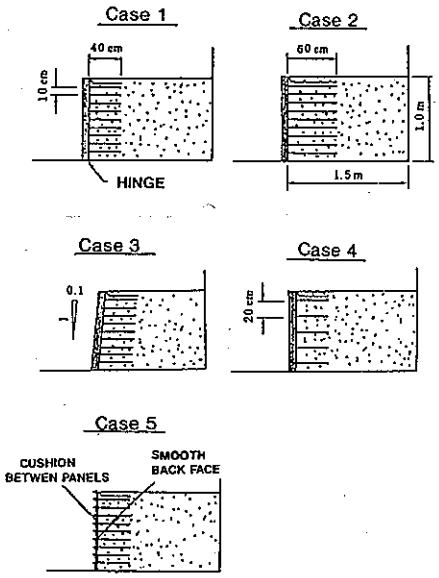

Case	Facing	NRL*	LR*	Slope of wall face	Note
1	one unit	10	40cm	Vertical	Standard
2	one unit	10	60cm	Vertical	Longer reinforcement
3	one unit	10	40cm	1:0.1(V:H)	Inclined facing
4	one unit	5	40cm	Vertical	Smaller NRL
5	discrete	10	40cm	Vertical	Less rigid facing

NRL: Number of reinforcement layers
LR : Length of reinforcement

Fig. 8 Models for dynamic loading tests.

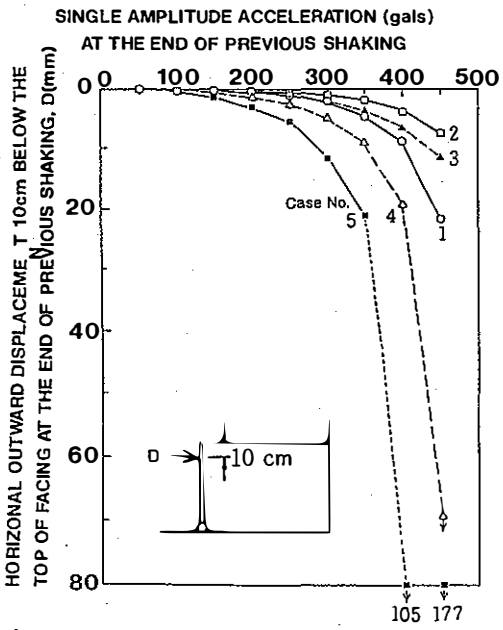

Fig. 9 Resuls of dynamic tests (Fig. 8).

that this type of GRS retaining wall can be designed so as to be stable enough against the design seismic load.

3 STABILITY ANALYSIS

Two-wedge stability analyses (Fig. 10) were performed, seeking the smallest safety factor by changing the locations of Points A and B and the angles θ_A and θ_B. Plane BE was assumed to be vertical. The effects of facing rigidity were taken into account in the following three ways: 1) For a continuous rigid facing Type D, Point A can be located only at the bottom level of facing (Fig. 11), whereas for flexible or incremental facings as Types A, B and C, Point A may be located at any level of facing. 2) Part of the weight of backfill can be transmitted to the facing through the shear force on the back face of facing (Fig. 12). The axial force V in the facing may be expressed as:

$$V = P \cdot \tan\phi_w, \qquad P = \alpha \cdot P_A \tag{1}$$

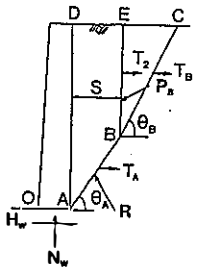

Fig. 10 Two-wedge stability analysis.

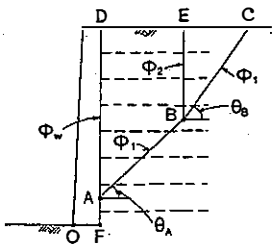

Fig. 11 Force components working in a GRS retaining wall.

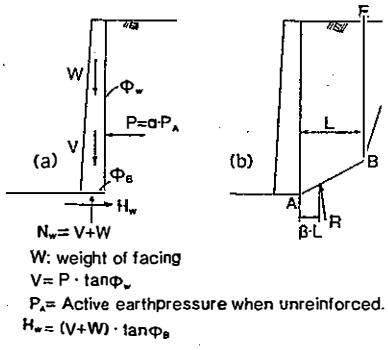

W: weight of facing
$V = P \cdot \tan\Phi_w$
P_A= Active earthpressure when unreinforced.
$H_w = (V+W) \cdot \tan\Phi_B$

Fig. 12 Coefficients α and β

where P is the total earth pressure activated on the back face of facing, ϕ_w is the wall friction angle and P_A is the active earth pressure activated on the back face of facing when the backfill is un-reinforced. The results of the laboratory and field tests showed that as the facing rigidity increases, the coefficient α increases from nearly zero for Type A to almost unity for Type D. 3) The test results also showed that as the facing rigidity increases, the location of the total reaction force (the sum of the reaction R on Plane AB and the vertical reaction N_W at the bottom of facing) becomes closer to the facing. This is due to the mechanism expressed by Eq. (1) and that the soil adjacent to the facing may become stronger as the facing rigidity increases due to the larger confining effect. The location of R is expressed as $\beta \cdot L$ (see Fig. 12b). These three mechanisms increase the stability of GRS retaining wall against sliding out and over-turning. This factor is ignored in most conventional limit equilibrium stability analyses.

The safety factor SF_S for sliding out along Plane AB was computed as:

$$SF_S = \{(S_{RW}+S_{RP}+S_{RT1}+S_{RT2}+S_{RNW}+S_{RHW}) / (F_{DW}+F_{DP})\}_{min} \quad (2)$$

where S_{RW} and S_{RP} are the shear strength of soil along Plane AB due to the weight of Block ABED and the earth pressure P_B activated on Plane BE, respectively, S_{RT1} is the component in the direction of Plane AB of the reinforcement force T_A activated between Points A and B, S_{RT2} is the shear strength of soil along Plane AB due to the increase in the normal stress caused by T_A, S_{RNW} and S_{RHW} are the components in the direction of Plane AB of the vertical reaction N_W and the shear force H_W, respectively, at the bottom of facing, and F_{DW} and F_{DP} are the disturbing forces due to the weight of Block ABDE and P_B, respectively. The safety factor SF_O for over-turning of the block ABED together with the facing about Point O was computed as:

$$SF_O = \{(M_{RW}+M_{RT1}) / (M_{DR}+M_{DP})\}_{min} \quad (3)$$

where M_{RW} is the resisting moment about Point O of the weight of Block ABED and facing, M_{RT1} is the resisting moment about Point O of the reinforcement forces T_A and T_2 (Fig. 11), M_{DR} and M_{DP} are the disturbing moment about Point O of the sum of R and N_W, and P_B. In this method, the reinforcement force increases the normal stress on the failure plane(s), thus, the soil shear strength. The smaller one of the above two safety factors is considered as the safety factor of wall.

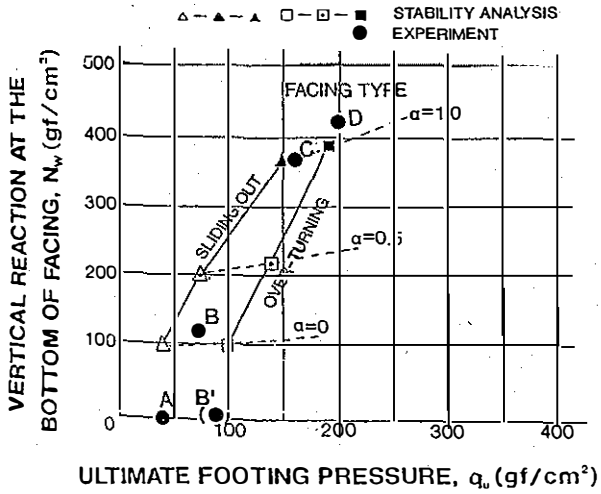

Fig. 13 Comparison of the results between model tests (Fig. 3a) and stability analysis.

For the laboratory tests (Fig. 3), the angle of internal friction of the backfill sand (Toyoura sand) by conventional plane strain compression (PSC) test was 49°. However, taking into account the effect of strength anisotropy and progressive failure, as the average friction angle mobilized along the failure plane at the moment of peak footing load, a reduced value ϕ = 43° was used. The average measured reinforcement force of 100gf/cm was used. The effect of the side wall friction estimated as 3gf/cm² was taken into account noting that the sand box width was 40cm. β = 0.4 was assumed for all the models, since values similar to 0.4 were observed for all the cases. In this case, the center of rotation was the center of facing base where the wooden block was supported on a hinge. The data points ● in Fig. 13 represent the measured maximum footing pressure q_u and the vertical reaction N_W at the facing bottom when q_u was activated for the case of back loading (Fig. 3a). The symbols ■, ⊡ and □ indicate the values of q_u and N_W for the case of over-turning estimated by the stability analysis using α = 1.0, 0.5 and 0.0, respectively. The symbols ▲, ◬ and △ are for the case of sliding out. The effect of α on both q_u and N_W is significant. For Type D, the estimated values of q_u and N_W for over-turning are very close to the measured values. This seems very reasonable, since the lowest block of the facings B, C and D was not allowed to translate by being supported on a hinge, thus the only possible failure mechanism for Type D was over-turning. For Type C, the estimated values for sliding out (α = 1.0) were very close to the measured values, which were smaller than the values for Type D. It is also reasonable, since the observed failure mechanism for Type C was nearly sliding out associated with the bending in the lower part of the facing which had only small overall bending rigidity. For Type B, both measured and estimated values are

Table 1 Summary of stability analysis for field loading tests (Fig. 7)

Test Segment	q_u (kgf/cm²) measured	estimated			
		α = 0.0	0.3	0.5	1.0
d (L= 2m)	6.0	3.1	-	4.1	5.8
f (L=1.5m)	5.5	3.0	-	4.0	5.5
h (L= 2m)	4.25	3.0	4.0	-	-

L: the length of reinforcement

much less than those for Types **C** and **D** with a low value of α (the measured and assumed values were 0.05 and 0.0), which resulted from its low facing rigidity. The observed failure mechanism was close to sliding out to a larger extent than for Type **C**. The observed value of N_w for Type **Λ** was plotted at zero by assuming α = 0.0 and by ignoring the weight of facing. The observed value of q_u for Type **Λ** was lower than that for Type **B**, due to the local failure which took place in the top soil layers. Since the estimated value of q_u for Type **Λ** for sliding out should be smaller than that for Type **B** due to the lack of facing weight, apparently, the analysis over-estimated the actual strength. For Type **B'**, the actual value of N_w may not be zero. Since the value was not measured, the data point was plotted arbitrarily at N_w= 0.0. A similar and consistent result was also obtained for the case of front loading (Fig. 3b).

In the analysis of the field test (Fig. 7), ϕ = 37.1° and c= 0.082 kgf/cm² obtained from PSC tests were used. The effect of progressive failure was ignored considering a small difference between the peak and residual strengths. This analysis seems less straightforward when compared with the above-mentioned case, because of some ambiguity in the side wall effect. A shear resistance between the test and control sections of 0.15 kgf/cm² was assumed with which all the field test results were well simulated. The measured reinforcement force of 300kgf/m and the assumed value β = 0.4 were used. For Segments **d** and **f** having a continuous rigid facing, the observed failure mechanism was over-turning, which was due to the effect of the resistance against sliding out of the buried part of facing. For the analysis of Segment **h**, only the observed failure mechanism, sliding out, was considered. For Segments d and f, the analysis underestimated the actual values when α =0.0 was used (Table 1), despite that the effects of strength anisotropy and progressive failure were ignored. This means that the actual value of α would be larger than 0.3. When using α =1.0, the estimated values of q_u were very similar to the measured values. For Segment h, α = 0.3 was estimated in such that the theoretical buckling strength of the discrete panels is 0.7kgf/m, which is 0.3 times the theoretical axial force activated in the facing at the peak footing load. By using α = 0.3, the measured value was well simulated. Considering some uncertainties in several assumed quantities, a very good agreement between the estimated and observed values may be somewhat fortuitous. However, it is obvious that also for this case, the effect of facing rigidity as observed could be estimated reasonably by the method described above. A similar and consistent result was also obtained for the static loading test No. 2 clay embankment. The effect of facing rigidity as observed in the dynamic model tests could also be well simulated by this analysis method.

4 CONCLUSIONS

For a geosynthetic-reinforced soil retaining wall, the use of continuous rigid facing was experimentally found to increase the stability of the wall. In stability analyses based on limit equilibrium formulation, the test results could be well explained only when taking into account the facing rigidity.

ACKNOWLEDGMENTS

The authors gratefully acknowledge Dr. H. Tarumi, Railway Technical Research Institute, Messrs. Nakamura, K. and Tamura, Y., Tokyu Construction Co., and Mr. K. Iwasaki, Mitsui Petrochemical Industry Ltd, for their support and cooperation.

REFERENCES

Murata, O., Tateyama, M, and Tatsuoka, F., Nakamura, K. and Tamura, Y. 1991. A reinforcing method for earth retaining walls using short reinforcing members and a continuous rigid facing, Proc. ASCE Geotech. Engrg Congress 1991, ASCE, Geotech. Special Publication 27: 935-946.

Tatsuoka, F., Tateyama, M. and Murata, O. 1989. Earth retaining wall with a short geotextile and a rigid facing, Proc. 12th ICSMFE, 2: 1311-1314.

Tatsuoka, F., Murata, O., Tateyama, M., Nakamura, K., Tamura, Y., Ling, H.I., Iwasaki, K. and Yamauchi, H. 1990. Reinforcing steep clay slopes with a non-woven geotextile, Proc. Int. Reinforced Soil Conf., Glasgow: 141-146.

Tatsuoka,F., Murata,O. and Tateyama,M. 1992. Permanent geosynthetic-reinforced soil retaining walls used for railway embankments in Japan, Proc. Int. Symp. on GRS retaining walls, Denver, Balkema.